Reuse of Spent Foundry Sand in Development of Glass-Ceramic Material with Wollastonite Phase

Renata da Silva Magalhães[a]* , Luis Fernando dos Santos[a] , Gleyson Tadeu de Almeida Santos[a],

Luiz Augusto Stuani Pereira[b], José Diego Fernandes[a], Agda Eunice de Souza Albas[a] ,

Silvio Rainho Teixeira[a]

[a]Universidade Estadual Paulista (UNESP), Departamento de Física, Roberto Simonsen 305, 19060-900, Presidente Prudente, SP, Brasil.
[b]Universidade Federal de Campina Grande (UFCG), Unidade Acadêmica de Física, Av. Aprígio Veloso, 882, Bodocongó, 58109-970, Campina Grande, PB, Brasil.

Spent Foundry Sand is one of the largest industrial solid wastes generated by foundries in the production of iron and steel components. Currently, millions of tons of molten sands are discarded worldwide. Therefore, this work aims to reuse the Spent Foundry Sand for the production of glass-ceramic materials, since this reuse minimizes the environmental impacts related to its discarding. The Spent Foundry Sand, composed of >60% SiO_2, was mixed with limestone and melted at 1500 °C to produce the glass (melting and rapid cooling method). The materials were characterized by X-Ray Fluorescence, X-Ray Diffraction and thermal analysis. The X-Ray Diffraction results of the glass tablets treated at 875, 941 and 1050 °C show that the formed phases are Wollastonite-1A, β-Wollastonite and Akermanite. In summary, it is possible to produce glass-ceramic from Spent Foundry Sand with Wollastonite phase.

Keywords: *Spent Foundry Sandy, Glass Ceramic, Wollastonite.*

1. Introduction

The foundry industry wastes, ferrous and non-ferrous metals, can be composed of several materials, such as Spent Foundry Sand (SFS), slag, ash, refractory, coagulant, powder, etc. Only the United States discards annually about 6 to 10 million tons of this type of waste, of which only 15% are recycled[1]. The foundry sector in Brazil has great participation in the world scenario, ranked ninth in the top 10 greatest powers, with a production of 2.28 million tons of castings in 2018[2]. According to Dyer et al.[3] a ton of molten material generates approximately 600 kg of SFS, thus Brazil provided around 1.37 million tons of SFS.

Consistent with ABNT NBR 10.004/2004[4], solid foundry waste is non hazardous and non inert. According to the standard the waste classified as hazardous (CLASS I) present reactivity, toxicity, flammability, corrosivity, and pathogenicity. On the other hand, the non-hazardous waste (CLASS II) is subdivided into: Class IIA – non-inert and Class IIB – inert. The present work makes use of the Class IIA – non inert waste, which can present characteristics such as biodegradability, combustibility or water solubility. The SFS have this label due to the binder used in the molding sands and the production process, whether ferrous or non-ferrous metals. Unfortunately, many companies do not use these suitable places and large amounts of SFS are incorrectly discarded in the environment. On the other hand, the proportion of waste that goes to licensed landfills demands high transportation and storage costs[5-6].

The United States is extremely strict with the use of SFS on the ground, since environmental agencies in several American states are concerned about the accumulation of metals and organic contaminants that can harm soil, plants and water[7]. Moreover, the US Environmental Protection Agency (USEPA) considers that 2% of the 10 million tons of SFS generated is classified as hazardous waste[8]. According to Winkler et al.[9] the deposit of SFS in industrial ladfills in the USA, for non-hazardous waste, has an approximate cost of US$ 15-75 per ton. This amount includes transportation, storage and labor, so it is estimated that the cost of depositing in landfills is between 100 and 250 million dollars per year.

Moreover, Bastian and Alleman[10] shows the SFS is not entirely an inert waste, which has contaminating potential according to the casting process. The reuse of SFS for glass-ceramic applications is an effective option for recycling the discarded waste, since you must first develop a glass to produce the glass-ceramic. The glass technology is advantageous for the waste incorporation as it immobilizes heavy metals through chemical bonds to a stable glass matrix, which considerably reduces the volume of the waste[11].

Most of the studies on waste from foundry industry focus on SFS[12], since it represents the largest waste generated by the foundry sector. Furthermore, a wide application is demonstrated in different works, such as in the manufacture of Portland cement and asphalt paving[1,13-14]. Even though studies have been carried out on the application of foundry waste with/without fragmentation and adding other types of waste in the composition[1-15], there is still a low number of published papers on the use of SFS in the development of glass-ceramic material.

*e-mail: r.s.magalhaes@hotmail.com

Silva et al.[16] showed the feasibility of using the SFS in place of pure silica in the manufacture process of glass-ceramics, however, the research used only SFS with phenolic resins. Zhang et al.[17] studied the glass matrix of a material manufactured through the sintering process by using foundry sand waste and glass waste as raw materials. The results indicate the material has the same performance as glass and ceramics, and therefore can replace natural stones.

The use of waste from the foundry industry as a precursor material for the development of glass-ceramics applied in civil constructions has numerous advantages, such as: saving raw materials, to improve the quality and reduce the cost of the final glass-ceramic material, in addition to reducing the environmental impacts caused by the sand extraction and discard of waste in the environment. The vitrification and crystallization process has been widely used to add value to inorganic waste of mining-industrial origin[14,18-19-20].

Many glass-ceramics with different compositions can be produced from the controlled crystallization of glasses. Wollastonite ($CaSiO_3$), for example, is the main crystalline phase of a glass-ceramic material commercially known as Neoparies®, which is manufactured from pure raw materials. This glass-ceramic is the first and most used due to its special properties in the civil construction, e.g. as coating for floors and walls[18]. This work aims to investigate the SFS recycling to obtain glass-ceramic materials with Wollastonite as a crystalline phase, that can be potentially applied in the civil construction sector i.e., coating commercial, industrial and residential floors and walls.

2. Materials and Methods

SFS was obtained from a foundry industry located in the region of Presidente Prudente, São Paulo state, Brazil. The foundry sand was characterized by X-Ray Fluorescence (XRF – Shimadzu EDX 7000) to determine the mass concentrations of oxides in the material. The analysis was carried out by inserting the sample in a polyester support, using a Rh anode as the excitation source, and an area of 10 mm² was analyzed. The sample was scanned in qualitative-quantitative mode, in the Na-U energy range and under vacuum at room temperature. Furthermore, the waste was submitted to X-Ray Diffraction analysis (Shimadzu XRD 6000) to determine its main crystalline phases.

The glass composition was obtained using the chemical formula of the Wollastonite phase ($CaSiO_3$) with a Si:Ca mole ratio of 1:1. The sample preparation was performed by mixturing SFS and limestone (Ca-Mg carbonate) (i.e., 35,8% of SFS and 64,2% of limestone from a total of 140 g). The theoretical glass melting temperature was calculated from the percentages of the compounds in the mixture using the method proposed by Chengyu and Ying[21] for silicate glasses.

The mixture was placed into an alumina crucible, which was 5 cm diameter and 10 cm height, and taken to the oven (SERVIFOR-1700 °C, SF-M220605 model) for melting during 1 h at 1500 °C. The liquid was poured into a container with distilled water at room temperature for the frit production.

The glass was grounded, passed through a 170 mesh sieve (<88 µm) and was characterized by thermal analysis equipment (TA Instruments, SDT Q600 model). The sample was analyzed under non-isothermal conditions, with a heating rate of 15 °C/min up to a temperature of 1300 °C, using an alumina crucible and synthetic air atmosphere with a flow rate of 100 mL/min. The thermal analysis (TG/DSC) was performed to determine the glass transition, crystallization and melting temperatures of the glassy material.

Afterwards, 0.5 g of the powder sample was used to make glass tablets, which were heat treated at temperatures of 875, 941 and 1050 °C (remaining 1 h at each temperature for crystallization to be evidenced). These temperatures correspond to the periods before, during and after the crystallization of the material.

The samples were analyzed using a Shimadzu XRD with the following characteristics: $CuK\alpha_1$ ($\lambda = 1.5406$ Å) and $CuK\alpha_2$ ($\lambda = 1.5444$ Å), voltage of 40 kV and current of 30 mA. They were scanned in the angular range 2θ from 10° to 80°, using divergence and reception slots with 1° opening in continuous mode, with a step of 0,02° and scanning speed of 2 °/min.

3. Results and Discussion

The XRF analysis shows the SFS chemical composition (oxide concentrations in mass percentage) consists mainly of silicon oxide and that limestone is mostly composed of calcium oxide (Table 1). These compounds are essential in the silicate glass manufacture, since SiO_2 forms the glass basic structure through the bonds between the oxygens in its tetrahedral. Moreover, CaO acts as a network modifier, i.e., it breaks the O-O bonds in the SiO_4^{-4} tetrahedrons, generating branches in the vitreous network and producing Ca^{2+} ions. However, because they are bivalent they chemically bond between the O⁻ branches[22,23,24]. In addition, the SFS – P has elements, such as Al_2O_3, Fe_2O_3 and MgO, whose concentrations are higher than in natural sand. This is associated with the bentonite (binding agent) insertion into the moulding sand[23,24,25,26].

Figure 1 shows the structural analysis of SFS – P by X-ray diffraction. The result indicate the material has Quartz (SiO_2) as a crystalline phase, which is one of the structures in highest concentration in the Earth's crust[22]. The Quartz has a hexagonal crystalline structure (PDF 5-490) that agrees with the XRF data.

Table 1. SFS and limestone chemical analyses (XRF mass %).

Oxides (%)	SiO_2	Al_2O_3	Fe_2O_3	SO_3	K_2O	Na_2O	CaO	MgO	TiO_2	LoI
SFS - P	67.1	14.6	2.9	2.2	0.6	---	1.7	2.0	0.6	8.3
Limestone	12.5	1.6	0.6	---	0.6	0.2	43.0	3.9	0.1	37.5
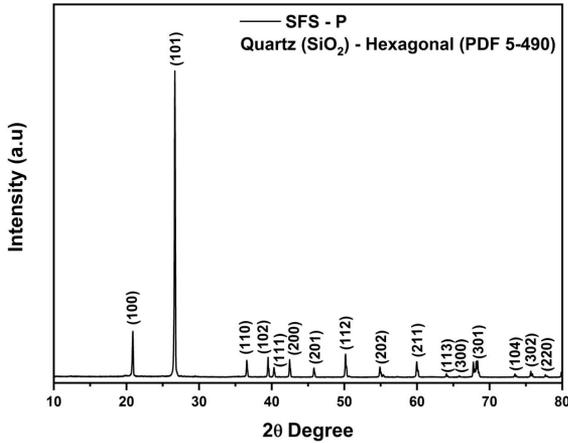
Figure 1. SFS – P structural analysis by X-ray diffraction.

Figure 2. SFS – P thermogravimetric analysis.

The SFS – P temperature thermogram (Figure 2) shows two unevennesses in the base line (green line), which are related to different thermal events. The first occurs at 200 °C and is associated with a small water loss (~0.7%), that is evidenced by the derivative thermogravimetric curve (DTG) in blue. The second reaction, between 200 and 700 °C with a value of 6.7%, is related to the bentonite decomposition and coal dust. It is worth saying both thermal events were also evidenced in Santos et al.[6] and Ahmad et al.[26].

The XRD characterization of limestone (Figure 3) shows crystalline planes associated with different compounds. One of the three observed crystalline phases is calcite ($CaCO_3$) in rhombohedral form (PDF 5-586), which is the main carbonate and sometimes the most predominant in sedimentary rocks[27]. Beyond this phase, dolomite ($CaMg(CO_3)_2$) in rhombohedral form (PDF 11-78) and Quartz in hexagonal form (PDF 5-490) are also present in the crystalline lattice. The XRD and XRF results show that CaO is the substance in greater quantity among the analyzed elements.

The thermogravimetric analysis of the limestone (Figure 4) shows the baseline changes slope in different regions of the thermogram. The first thermal event associated with moisture loss occurs up to 200 °C followed by a second loss between the temperatures of 200 and 650 °C, which is related to the magnesium carbonate decomposition releasing CO_2. Similarly, the third thermal event is associated with decomposition, however, the dissociated substance is calcium carbonate and the baseline changes slope between the temperatures of 650 and 900 °C. Both substances undergo decomposition and release CO_2 in the formation of magnesium and calcium oxides[28].

Table 2 presents the oxide values in mass percentage that form glassy materials. As previously mentioned, silicate glass was obtained through the oxygen bonds in the $(SiO_4)^{4-}$ tetrahedral forming a three-dimensional structure.
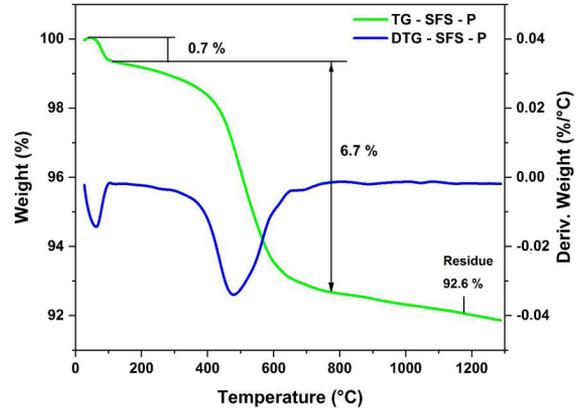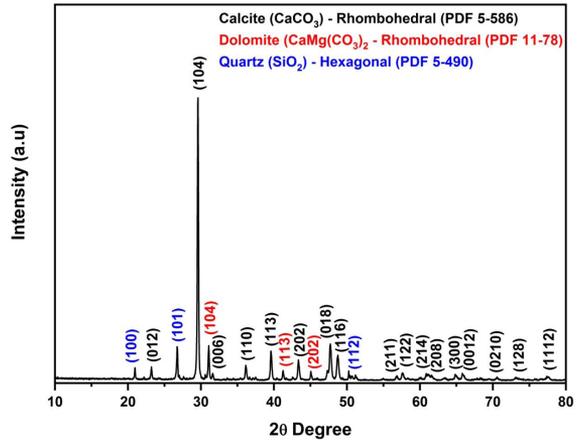
Figure 3. Limestone analysis by X-ray diffraction.
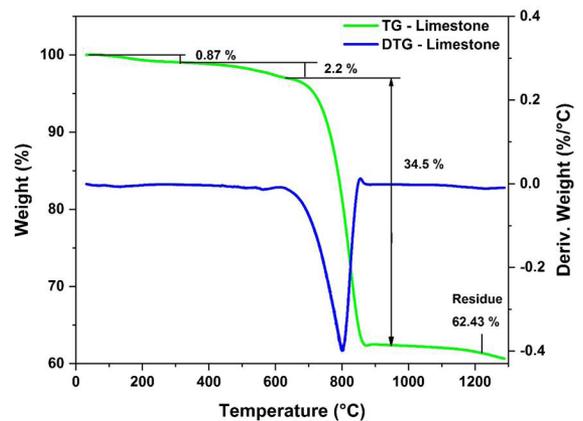
Figure 4. Limestone thermogravimetric analysis.

Table 2. Glass – P chemical analysis (XRF mass %).

Oxides (%)	SiO_2	Al_2O_3	Fe_2O_3	SO_3	K_2O	CaO	MgO	TiO_2
Glass - P	48.2	5.4	1.1	0.1	0.6	41.2	3.3	0.1

The divalent ions (Ca^{2+} and Mg^{2+}), called network modifiers, bonded ionically to the $(SiO_4)^{4-}$ tetrahedral to compensate for the negative charges[22,23,24]. The aluminum oxide (Al_2O_3) is another substance in the glass and SFS compositions that was analyzed by the XRF technique. This substance acts as a network stabilizer, decreasing the devitrification and increasing the composition's viscosity[23,24,29,30].

The mass percentages of the two main oxides (SiO_2 and CaO) in the glass were calculated to obtain a composition that after heating a glass-ceramic material is produced with Wollastonite crystalline phase.

The glass XRD analysis (Figure 5) shows a broad and diffuse band around $2\theta = 30$ °, which is a characteristic of non-crystalline materials that have SiO_2 as a glassy network. According to the literature, the glasses have a topologically-disordered network and do not have long-range order within the atomic structure. When cooling is applied they present imperceptible crystalline volumetric fractions and thus the glassy structure is non-crystalline when analyzed via XRD[31].

The differential scanning calorimetry (DSC) of glass – P (Figure 6) shows thermal reactions occurring in different regions. The baseline changes slope at 640 °C, which is related to the glass transition (T_g) followed by the initial crystallization temperature (T_x) at 880 °C, the peak temperature (T_c) at 941 °C and the melting temperature (T_m) at 1199 °C.

The thermal transitions are theoretically associated with: i) the material structural relaxation at temperatures around T_g; ii) T_c to the rearrangement caused by the loss of molecular stability, moving from a non-crystalline to a more stable crystalline structure; and iii) T_m represents the maximum temperature in which crystals can coexist with the melting mass obeying the thermodynamic equilibrium[18-24].

Figure 7 shows the X-ray diffraction data of the heat-treated pellets at 875, 941 and 1050 °C, which correspond to the pattern of the glass-ceramic material. The formation of the Wollastonite phase was observed, which theoretically has different properties, e.g. hardness between 4.5 and 5 on the Mohs scale, glassy appearance, low moisture and oil absorption, and low volatile content. Therefore, the industries commercialize materials with this crystalline phase for different sectors, e.g. the civil construction (floor and wall covering) and friction products (brakes and/or clutches)[32].

Owing to the impurity content in glass-ceramic materials secondary phases can occur. The presence of the impurities influenced the formation of the Akermanite phase ($Ca_2Mg(Si_2O_7)$), which is a calcium and magnesium silicate that has hardness between 5 and 6 on the Mohs scale, gray, green, yellowish colors or it can even be colorless depending on the colored ion content in the material; moreover, it has a glassy appearance[33]. When this silicate is produced with pure raw materials, it is used as dental and bone implants[34,35].

The aluminum oxide (Al_2O_3) did not form noticeable crystalline phases in the XRD analysis, although, it was significantly present in the XRF analysis. This can be attributed to the large amount of this oxide in the glassy phase, which does not contribute to the formation of nuclei and, consequently, crystals. Since, the Al^{3+} ions need to replace the Si^{4+} to form secondary structures, alkaline and alkaline-earth atoms migrate to the interstices to compensate for the charges in the structure[22-30].
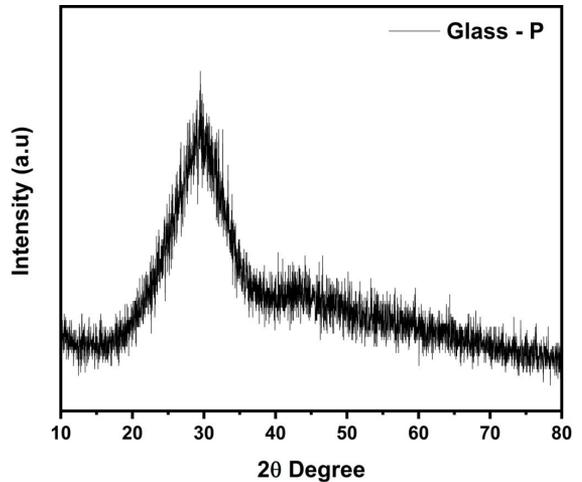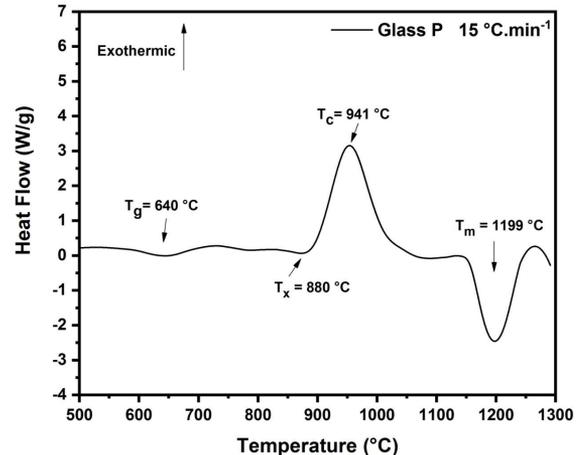

Figure 5. Glass – P X-ray diffraction.

Figure 6. DSC analysis of glass – P with scanning at 15°C/min up to 1300°C.

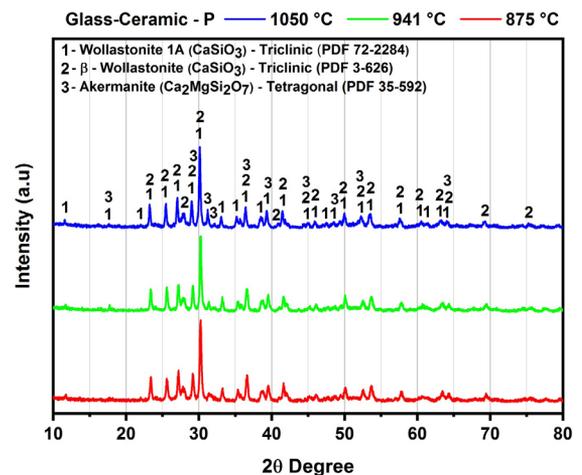**Figure 7.** X-ray diffraction of the heat-treated tablets (glass-ceramic – P) at 875, 941 and 1050 °C.

Teixeira et al.[36] showed that the glass-ceramic with Wollastonite as the main crystalline phase has hardness and the characteristics that make it useful to replace decorative stones, e.g. marble and granite, in civil construction.

The pellets with heat treatment at temperatures of 875, 941 and 1050 °C (using the DSC data) (Figure 8) have different colors. The P-glass has an apparently light green color, while the glass-ceramic inserts vary from green to yellow. This is due to the presence of coloring ions such as iron and titanium. The ions that color glasses do not always display the same color as it is associated with the ion type, its valence number and how this interaction occurs in the glassy or crystalline structure. In addition, an ion can have different colors depending on the electronic vibration intensity as well as the presence of local crystal defects, which are known as color centers[37].

Table 3 shows the results of Vickers microhardness analysis of the P glass-ceramic. The hardness varies with increasing temperature, which is associated with the different phases present in the material as they have different hardness values. The property (hardness) analyzed in the P glass-ceramic exhibits values similar to commercial glass-ceramics. Another fact is that it has a higher hardness than marble and granite[36]. The material visual (Figure 8) is very attractive. Even, with a satisfactory improvement, it can be used to coat industrial, commercial and residential floors and walls.

Romero et al.[38] used municipal incinerator waste to obtain glass-ceramics and showed that the Arkemanite phase exhibits a Vickers microhardness of 6.6 ± 0.2 GPa. Peng et al.[39] produced glass-ceramics with Wollastonite phase using coal ash and obtained microhardness between 5.4 and 6.9 GPa. In 2005, they[40] used Wollastonite and Anorthite phases and got microhardness from 5.2 to 7.1 GPa. Ferreira et al.[41] produced a glass-ceramic material with metallurgical slag with Wollastonite and Augite phases and obtained a microhardness of 7.8 ± 0.2 GPa.

These data reveal that the glass-ceramics developed in this work have values similar to those found in the literature.
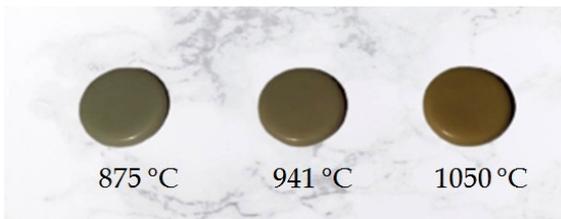
Figure 8. Glass tablets with heat treatment at temperatures of 875, 941 and 1050 °C.

Table 3. Microhardness analysis, HV and GPa, the Glass Ceramic P

	Hardness - HV	Hardness - GPa
Glass Ceramic P – 875 °C	(70 ± 7) x10	6.91 ± 0.7
Glass Ceramic P – 941 °C	(68 ± 5) x10	6.69 ± 0.5
Glass Ceramic P – 1050 °C	(73 ± 3) x10	7.18 ± 0.3

4. Conclusion

In this study, it was shown that SFS can be recycled to produce glass-ceramic materials with Wollastonite ($CaSiO_3$) as the main crystalline phase. The X-ray diffraction results of the glass tablets with heat treatment at 875, 941 and 1050 °C shows the formation phases are: Wollastonite-1A, β-Wollastonite and Akermanite. It is worth mentioning glass-ceramic material is produced at low cost, since limestone is a cheap material. This glass-ceramic has special properties which make it potentially applied in the civil construction, e.g. as coating for floors and walls.

5. Acknowledgements

6. References

1. Torres A, Bartlett L, Pilgrim C. Effect of foundry waste on the mechanical properties of Portland Cement Concrete. Constr Build Mater. 2017;135:674-81.
2. Modern Casting. Census of world casting production. Schaumburg: American Foundry Society; 2018.
3. Dyer PPOL, Lima MG, Klinsky LMG, Silva SA, Coppio GJL. Environmental characterization of Foundry Waste Sand (WFS) in hot mix asphalt (HMA) mixtures. Constr Build Mater. 2018;171:474-84.
4. ABNT: Associação Brasileira de Normas Técnicas. ABNT NBR 10004: resíduos sólidos: classificação. Rio de Janeiro: ABNT; 2004.
5. Siddique R, Schutter G, Noumowe A. Effect of used-foundry sand on the mechanical properties of concrete. Constr Build Mater. 2009;23(2):976-80.
6. Santos LF, Magalhães RS, Barreto SS, Santos GTA, Paiva FFG, Souza AE et al. Characterization and reuse of spent foundry sand in the production of concrete for interlocking pavement. J Build Eng. 2021;36:1-7.
7. Stehouwer RC, Hindman JM, Macdonald KE. Nutrient and trace element dynamics in blended topsoils containing spent foundry sand and compost. J Environ Qual. 2009;39(2):587-95.
8. USEPA – United States Environmental Protection Agency [Internet]. Beneficial reuse of foundry sand: a review of state practices and regulations. Washington, DC: USEPA; 2002 [cited 2023 Jun 18]. Available from: https://nepis.epa.gov/Exe/ZyPDF.cgi/9101ZMM6.PDF?Dockey=9101ZMM6.PDF
9. Winkler E, Kosanovic B, Genovese T, Roth I. A survey of foundry participation in the Massachusetts beneficial use determination process. Chelsea: Chelsea Center for Recycling and Economic Development; 1999.
10. Bastian KC, Alleman JE. Microtox (TM) characterization of foundry sand residuals. Waste Manag. 1998;18(4):227-34.
11. Colombo P, Brusatin G, Bernardo E, Scarinci G. Inertization and reuse of waste materials by vitrification and fabrication of glass based products. Curr Opin Solid State Mater Sci. 2003;7(3):225-39.
12. Winkler ES, Bol'Shakov AA. Characterization of foundry sand waste. Chelsea: Chelsea Center for Recycling and Economic Development; 2000.

13. Pasetto M, Baldo N. Recycling of waste aggregate in cement bound mixtures for road pavement bases and sub-bases. Constr Build Mater. 2016;108:112-8.

14. Arulrajah A, Yaghoubi E, Imteaz M, Horpibulsuk S. Recycled waste foundry sand as a sustainable subgrade fill and pipe-bedding construction material: engineering and environmental evaluation. Sustain Cities Soc. 2017;28:343-9.

15. Mymrin V, Alekseev K, Catai RE, Nagalli A, Aibuldinov YK, Bekturganov NS et al. Red ceramics from composites of hazardous sludge with foundry sand, glass waste and acid neutralization salts. J Environ Chem Eng. 2016;4:753-61.

16. Silva LMS, Magalhães RS, Macedo WC, Santos GTA, Albas AES, Teixeira SR. Utilization of discarded foundry sand (DFS) and inorganic waste from cellulose and paper industry for the manufacture of glass-ceramic materials. Cerâmica. 2020;66:413-20.

17. Zhang Z, Xia J, Zhu X, Liu F, He M. Glass matrix composite material prepared with waste foundry sand. China Foundry. 2006;3(4):279-83.

18. Höland W, Beall G, editors. Glass-ceramic technology. Westerville: The American Ceramic Society Publishing; 2002.

19. Rawlings RD, Wu JP, Boccaccini AR. Glass-ceramics: their production from wastes - a review. J Mater Sci. 2006;41:733-61.

20. Andreola F, Barbieri L, Lancellotti I, Leonelli C, Manfredini T. Recycling of industrial wastes in ceramic manufacturing: state of art and glass case studies. Ceram Int. 2016;42:13333-8.

21. Chengyu W, Ying T. Calculation of the melting temperatures of silicate glasses. Glass Technol. 1983;24(5):278-82.

22. Kingery WD, Bowen HK, Uhlmann DR, editors. Introduction to ceramics. Medford: John Wiley & Sons Publishing; 1976.

23. Zarzycki J. Glasses and the vitreous state. New York: Cambridge University Press; 1991.

24. Callister WD, Rethwisch DG, editors. Fundamentals of materials science and engineering: an integrated approach. 5th ed. Hoboken: Wiley; 2015.

25. Çevik S, Mutuk T, Oktay BM, Demirbas AK. Mechanical and microstructural characterization of cement mortars prepared by waste foundry sand (WFS). J. Australas. Ceramic Society. 2017;53:829-37.

26. Ahmad HM, Kamal MS, Al-Harthi MA. Effect of thermal aging and electrolyte on bentonite dispersions: rheology and morphological properties. J Mol Liq. 2018;269:278-86.

27. Robinson SM, Santini K, Moroney J. Wollastonite. In: Kogel JE, Trivedi NC, Barker JM, Krukowsk ST, editors. Industrial minerals and rocks: commodities, markets and uses. Littleton: Society for Mining, Metallurgy, and Exploration, Inc; 2009. p. 1027-37.

28. Caceres PG, Attiogbe EK. Thermal decomposition of dolomite and the extraction of its constituents. Miner Eng. 1997;10(10):1165-76.

29. Allix M, Cormier L. Les vitrocéramiques. Tech Ing. 2013;4(802):1-26.

30. Rincón JM. Principles of nucleation and controlled crystallization of glasses. Polym Plast Technol Eng. 1992;31(3-4):309-57.

31. Gupta PK. Non-crystalline solids: glasses and amorphous solids. J Non-Cryst Solids. 1996;195:158-64.

32. Maxim LD, McConnell EE. A review of the toxicology and epidemiology of wollastonite. Inhal Toxicol. 2005;17:451-66.

33. Anthony JW, Bideaux RA, Bladh KW, Nichols MC, editors. Handbook of mineralogy. Tucson: Mineral Data Publishing; 1990.

34. Ventura JMG, Tulyaganov DU, Agathopoulos S, Ferreira JMF. Sintering and crystallization of akermanite-based glass–ceramics. Mater Lett. 2006;60:1488-91.

35. Marzban K, Rabiee SM, Zabihi E, Bagherifard S. Nanostructured akermanite glass-ceramic coating on Ti6Al4V for orthopedic applications. J Appl Biomater Funct Mater. 2019;17(2):1-8.

36. Teixeira SR, Souza AE, Carvalho CL, Reynoso VCS, Romero M, Rincón JM. Characterization of a wollastonite glass-ceramic material prepared using sugar cane bagasse ash (SCBA) as one of the raw materials. Mater Charact. 2014;98:209-14.

37. Karmakar B, editor. Functional glasses and glass-ceramics: processing, properties, and applications. Oxford: Elsevier; 2017.

38. Romero M, Rawlings RD, Rincón JM. Crystal nucleation and growth in glasses from inorganic wastes from urban incineration. J Non-Cryst Solids. 2000;271:106-18.

39. Peng F, Liang K, Hu A, Shao H. Nano-crystal glass-ceramics obtained by crystallization of vitrified coal fly ash. Fuel. 2004;83(14-15):1973-7.

40. Peng F, Liang K, Hu A. Nano-crystal glass-ceramics obtained from high alumina coal fly ash. Fuel. 2005;84:341-6.

41. Ferreira EB, Zanotto ED, Scudeller LAM. Glass and glass-ceramic from basic oxygen furnace (BOF) slag. Glass Sci Technol. 2002;75(2):75-86.